The Intra- and Intermolecular Oxidative Coupling of Ni(II)-*meso*-Octaethyl Mono(pyridine)−Tris(pyrrole) Complex Leading to C−C Bonds: Pathways to Oligomeric Porphyrinogens

Raffaella Crescenzi, Euro Solari, and Carlo Floriani*

Institut de Chimie Minérale et Analytique, BCH, Université de Lausanne, CH-1015 Lausanne, Switzerland

Angiola Chiesi-Villa and Corrado Rizzoli

Dipartimento di Chimica, Università di Parma, I-43100 Parma, Italy

Received June 10, 1998

This paper reports the oxidative transformations of the unprecedented *meso*-octaalkyl mono(pyridine)−tris(pyrrole) macrocycle $[Et_8(C_5H_3N)(C_4H_2NH)_3]$, **1**, which was obtained by a homologation of the corresponding porphyrinogen, $[Et_8(C_4H_2NH)_4]$, **A**. The metallation of **1** was obtained via its deprotonation with LiBu, followed by the reaction with $MCl_2{\cdot}thf_n$, leading to the bimetallic complexes: $[Et_8(C_5H_3N)(C_4H_2N)_3M\{Li(thf)_2\}]$ [M = Fe, **3**; M = Co, **4**; M = Ni, **6**; M = Cu, **7**]. The cobalt derivative occurs also in the separated ion-pair form $[Et_8(C_5H_3N)(C_4H_2N)_3Co]^-$-$[\{Li(thf)_4\}]^+$, **5**. The reaction of **4** and **6** with an excess of Cp_2FeBPh_4 led to the oxidation of the macrocycle with the formation of a cyclopropane functionality $[Et_8(C_5H_3N)\{(C_4H_2N)_3(\Delta)\}Ni]^+BPh_4^-$, **8**. The cyclopropane unit underwent reductive cleavage back to the initial macrocycle using lithium metal. The use of a Ni/Cp_2Fe^+ 1:1 ratio allowed the identification of a dimer derived formally from the monoelectronic oxidation of the macrocycle **1**, which formed a radical coupling to **9**, $[Et_8(C_5H_3N)(C_4H_2N)_3Ni]_2$. The same compound formed from a disproportionation redox reaction occurring between **6** and **8**. The C−C bond across the two metallamacrocycles involved the β position of the pyrrole. Deprotonation of **9** by LiBu led to a dianionic form **10** $[Et_8(C_5H_3N)(C_4H_2N)_3$-$Ni\{Li(thf)_2\}]$. The formation of the cyclopropane functionality was also achieved via the oxidation of $[Et_8(C_5H_3N)(C_4H_2N)_3Li_3(thf)_2]$, **2**, forming $[Et_8(C_5H_3N)\{(C_4H_2N)_3(\Delta)\}Li(thf)]$, **11**, which was ready to be used in metallation reaction. The proposed structures were supported by X-ray analyses on **4**, **7**, **8**, **9**, and **11**.

Introduction

The redox chemistry of macrocyclic complexes is a major synthetic and mechanistic field in coordination chemistry.[1] The macrocyclic ligand affects the redox potential of the transition metal, without undergoing any chemical change. Much more rarely the redox reactions cause modifications in the macrocyclic ligand without affecting the oxidation state of the metal.[2] In the most interesting cases, they either occur independently or can couple. This type of two parallel redox behavior is displayed by the so-called artificial porphyrins,[3] which are oxidized forms of porphyrinogen other than porphyrins. We report here the redox behavior of a modified form of the *meso*-octaethylporphyrinogen, in which one of the pyrrole rings has been replaced by a pyridine (Chart 1). The ligand **B** has been obtained with an organometallic methodology enabling **B** to be obtained directly from the corresponding *meso*-octaethylporphyrinogen **A** via the homologation of a single pyrrole (Chart 1).[4] The presence of a pyridine ring would change both the redox properties of the ligand and its relationship with the metal. In this paper we will examine the metallation of the ligand **B** using Fe(II), Co(II), Ni(II), and Cu(II), and the structural properties of the resulting complexes, along with the chemical

Chart 1

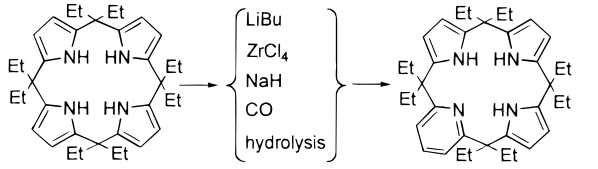

$[Et_8N_4H_4]$, **A** $[Et_8(C_5H_3N)(C_4H_2NH)_3]$, **B**

* To whom correspondence should be addressed.

(1) Dietrich, B.; Viout, P.; Lehn, J.-M. *Macrocyclic Chemistry*; VCH: Weinheim, Germany, 1993. Lindoy, L. F. *The Chemistry of Macrocyclic Ligand Complexes*; Cambridge University Press: Cambridge, U.K., 1989.

(2) Gallo, E.; Solari, E.; Re, N. Floriani, C.; Chiesi-Villa, A.; Rizzoli, C. *J. Am. Chem. Soc.* **1997**, *119*, 5144 and references therein.

(3) (a) Floriani, C. *Chem. Commun.* **1996**, 1257. (b) De Angelis, S.; Solari, E.; Floriani, C.; Chiesi-Villa, A.; Rizzoli, C. *J. Am. Chem. Soc.* **1994**, *116*, 5691. (c) De Angelis, S.; Solari, E.; Floriani, C.; Chiesi-Villa, A.; Rizzoli, C. *J. Am. Chem. Soc.* **1994**, *116*, 5702. (d) Floriani, C. In *Transition Metals in Supramolecular Chemistry*; Fabbrizzi, L., Poggi, A., Eds.; Kluwer: Dordrecht, The Netherlands, 1994; Vol. 448, p 191. (e) Piarulli, U.; Solari, E.; Floriani, C.; Chiesi-Villa, A.; Rizzoli, C. *J. Am. Chem. Soc.* **1996**, *118*, 3634.

(4) (a) Jacoby, D.; Floriani, C.; Chiesi-Villa, A.; Rizzoli, C. *J. Am. Chem. Soc.* **1993**, *115*, 7025. (b) Jacoby, D.; Isoz, S.; Floriani, C.; Chiesi-Villa, A.; Rizzoli, C. *J. Am. Chem. Soc.* **1995**, *117*, 2793. (c) Floriani, C. In *Stereoselective Reactions of Metal-Activated Molecules*; Werner, H., Sundermeyer, J., Eds.; Vieweg: Wiesbaden, 1995; pp 97−106. (d) De Angelis, S.; Solari, E.; Floriani, C.; Chiesi-Villa, A.; Rizzoli, C. *Organometallics* **1995**, *14*, 4505. (e) Isoz, S.; Floriani, C.; Schenk, K.; Chiesi-Villa, A.; Rizzoli, C. *Organometallics* **1996**, *15*, 337. (g) Floriani, C. *Pure Appl. Chem.* **1996**, *68*, 1.

10.1021/ic9806378 CCC: $15.00
Published on Web 10/22/1998

changes occurring on the ligand upon oxidation. The latter reaction leads, dependent on the reaction conditions, to the formation of intramolecular or intermolecular C−C bonds, which behave differently under reductive conditions. The formation of intermolecular C−C bonds exemplifies how we can manage the oxidation of the porphyrinogen-type skeleton to some oligomeric forms. The model compounds which were used for investigating the redox behavior of the *meso*-octaethyl mono(pyridine)−tris(pyrrole) macrocycle are the lithium and the Ni^{II}−Li derivatives.

Experimental Section

General Procedure. All reactions were carried out under an atmosphere of purified nitrogen. Solvents were dried and distilled before use by standard methods. Infrared spectra were recorded with a Perkin-Elmer FT 1600 spectrophotometer, UV-vis spectra were recorded with a Hewlett-Packard 8452A diode array spectrophotometer, NMR spectra were recorded on AC-200E and DPX-400 Bruker instrument. Magnetic susceptibility measurements were collected on a MPMS5 SQUID apparatus (Quantum Design Inc.). Corrections were applied for diamagnetism calculated from Pascal constants. The synthesis of **1** and **2** was carried out as reported.[4b]

Synthesis of 3. $[FeCl_2(thf)_{1.5}]$ (1.81 g, 7.71 mmol) was added to a THF (125 mL) solution of **2** (5.51 g, 7.71 mmol) at room temperature. The resulting purple solution which was allowed to stand for 20 h. The solvent was removed under reduced pressure, the solid collected with diethyl ether (200 mL) and extracted to remove LiCl. The mother liquor was concentrated, and the orange product was filtered and dried (5.1 g; 88%). Anal. Calcd for $C_{45}H_{65}FeLiN_4O_2$: C, 71.38; H, 8.66; N, 7.40. Found: C, 71.67; H, 8.70; N, 7.20. IR (nujol, ν_{max}/cm^{-1}): 3094 (s) 1594 (s), 1568 (s), 1321 (m), 1244 (w), 1194 (w), 1154 (w), 1064 (s), 1035 (s), 887 (m), 857 (m), 765 (s), 737 (s). $\mu_{eff} = 3.88\ \mu_B$ at 293 K.

Synthesis of 4. $[CoCl_2(thf)_{1.5}]$ (2.42 g, 10.2 mmol) was added to a THF (150 mL) solution of **2** (7.27 g, 10.2 mmol). The resulting red solution was allowed to stand for 24 h. The solvent was removed under reduced pressure, the yellow solid collected with diethyl ether (150 mL) and extracted to remove LiCl. The mother liquor was concentrated, and the yellow product was filtered and dried (5.7 g; 73%). Anal. Calcd for $C_{45}H_{65}CoLiN_4O_2$: C, 71.13; H, 8.62; N, 7.37. Found: C, 70.69; H, 8.46; N, 7.65. IR (nujol, ν_{max}/cm^{-1}): 3078 (s), 1594 (s), 1561 (s), 1322 (m), 1033 (s), 889 (s), 755 (s), 717 (m). $\mu_{eff} = 2.75\ \mu_B$ at 293 K. The recrystallization of **4** from thf−hexane led to crystals suitable for the X-ray analysis. They are a differently solvated form of **4** containing the separated ion-pair form $[Et_8(C_5H_3N)(C_4H_2N)_3Co]^-[Li(thf)_4]^+$, **5**.

Synthesis of 6. $[NiCl_2(thf)]$ (2.5 g, 12.0 mmol) was added to a THF (150 mL) solution of **2** (9.03 g, 12 mmol). The resulting red solution was allowed to stand for 24 h. The solvent was removed under reduced pressure, and the solid was collected with diethyl ether (180 mL) and extracted to remove LiCl. The mother liquor was evaporated to dryness, and the yellow product was collected with *n*-hexane (100 mL), filtered and dried (6.5 g; 70%). Anal. Calcd for **6**, $C_{45}H_{65}LiN_4NiO_2$: C, 71.15; H, 8.62; N, 7.38. Found: C, 70.65; H, 8.88; N, 7.37. IR (Nujol, ν_{max}/cm^{-1}): 3077 (w), 1595 (s), 1569 (s), 1394 (m), 1323 (w), 1269 (w), 1158 (w), 1064 (s), 1037 (s), 887 (m), 765 (s), 728 (s). ^1H NMR (CD_3COCD_3, 200 MHz, 298 K, ppm): δ 7.64 (t, $J = 7.8$ Hz, 1H, C_5H_3N); 7.26 (d, $J = 7.8$ Hz, 2H, C_5H_3N); 5.57 (d, $J = 2.9$ Hz, 2H, C_4H_2N); 5.50 (d, $J = 2.9$ Hz, 2H, C_4H_2N); 5.45 (s, 2H, C_4H_2N); 4.62−3.58 (s br, 4H, CH_2); 3.62 (m, 8H, THF); 2.87 (q, $J = 7.3$ Hz, 4H, CH_2) 2.27 (q, $J = 7.3$ Hz, 4H, CH_2); 1.97 (m, 4H, CH_2); 1.79 (m, 8H, THF); 1.08 (m, 12H, CH_3); 0.69 (t, $J = 7.3$ Hz, 12H, CH_3).

Synthesis of 7. $[CuCl_2(thf)_{0.5}]$ (2.38 g, 14.0 mmol) was added to a THF (150 mL) solution of **2** (10.23 g, 14.90 mmol). The resulting red solution was allowed to stand for 24 h. The solvent was removed under reduced pressure, and the solid was collected with diethyl ether (120 mL) and extracted to remove LiCl. The mother liquor was evaporated to dryness and the product collected with *n*-hexane (100 mL), filtered and dried (7.5 g; 70%). Crystals suitable for X-ray analysis were obtained by very slowly extracting the raw product with diethyl ether. Anal. Calcd for **7**, $C_{45}H_{65}CuLiN_4O_2$: C, 70.73; H, 8.57; N, 7.33. Found: C, 70.63; H, 8.66; N, 7.37. IR (Nujol, ν_{max}/cm^{-1}): 3078 (s), 1591 (s), 1570 (s), 1321 (m), 1074 (m), 1038 (s), 887 (s), 765 (s), 738 (s). $\mu_{eff} = 1.77\ \mu_B$ at 293 K.

Synthesis of 8. Cp_2FeBPh_4 (4.21 g, 8.3 mmol) was added to a yellow solution of **6** (1.43 g, 2.1 mmol) in THF (120 mL), cooled at −40 °C. The resulting red solution was then allowed to warm up to room temperature and it was left standing for 24 h. Solvent was evaporated under reduced pressure and the red residue collected and extracted with *n*-hexane (120 mL) to remove $[Cp_2Fe]$. The residue was dried, dissolved in THF (∼50 mL) and precipitated with *n*-hexane (∼120 mL), then filtered and dried (1.33 g, 63%). Crystals suitable for X-ray analysis were grown in DME and do not contain thf of crystallization. Anal. Calcd for **8**·thf, $C_{65}H_{77}BN_4NiO$: C, 78.13; H, 7.71; N, 5.61. Found: C, 78.41; H, 7.71; N, 5.74. IR (Nujol, ν_{max}/cm^{-1}): 3088 (s), 1938 (w), 1872 (w), 1811 (w), 1624 (m), 1577 (s), 1304 (w), 1266 (s), 1127 (w), 1081 (s), 1029 (s), 798 (s), 765 (s), 738 (s), 701 (s). ^1H NMR (CD_2Cl_2, 400 MHz, 298 K, ppm): δ 7.87 (t, $J = 7.8$ Hz, 1H, C_5H_3N); 7.61 (d, $J = 7.8$ Hz, 1H, C_5H_3N); 7.46 (m, 2H, C_4H_2N); 7.39 (d, $J = 7.8$ Hz, 1H, C_5H_3N); 7.35 (m, 8H, BPh_4); 7.04 (m, 8H, BPh_4); 6.90 (m, 4H, BPh_4) 6.84 (d, $J = 5.2$ Hz, 1H, C_4H_2N); 6.74 (d, $J = 5.2$ Hz, 1H, C_4H_2N); 6.08 (d, $J = 3.2$ Hz, 1H, C_4H_2N); 5.86 (d, $J = 3.2$ Hz, 1H, C_4H_2N); 4.51 (m, 1H, CH_2); 3.94 (m, 1H, CH_2); 3.11 (m, 1H, CH_2); 2.65−2.44 (m, 3H, CH_2); 2.27−2.19 (m, 5H, CH_2); 1.97−1.93 (m, 5H, CH_2); 1.14 (t, $J = 7.2$ Hz, 3H, CH_3); 0.98−0.93 (m, 12H, CH_3); 0.90 (t, $J = 7.2$ Hz, 3H, CH_3); 0.52 (m, 3H, CH_3); 0.48 (t, $J = 7.2$ Hz, 3H, CH_3).

Reduction of 8 to 6 with Li. Metal lithium (0.029 g; 4.2 mmol) and degassed biphenyl (0.008 g) were added to the yellow solution of **8** (1.16 g, 1.16 mmol) in THF (70 mL) under argon. The suspension was stirred at room temperature for 24 h, excess Li was then filtered off, and the solvent was evaporated to dryness. The green-yellow solid was collected with *n*-hexane (100 mL) and extracted. The mother liquor was concentrated, and the solid was filtered and dried. The ^1H NMR spectrum was identical to that of **6**.

Synthesis of 9. $[Cp_2FeBPh_4]$ (3.86 g, 7.6 mmol) was added to an orange solution of **6** (5.25 g, 7.6 mmol) in THF (150 mL), cooled at −40 °C. The resulting red solution was warmed up to room temperature and kept on standing overnight. The solvent was evaporated at reduced pressure, and the solid was collected with *n*-hexane (100 mL) and then extracted with *n*-hexane (120 mL). The mother liquor was concentrated and the residue solid filtered and dried (3.1 g; 67%). Crystals suitable for the X-ray analysis were obtained from DME and contain DME of crystallization. Anal. Calcd for **9**, $C_{74}H_{98}N_8Ni_2$: C, 73.03; H, 8.11; N, 9.2. Found: C, 72.92; H, 8.18; N, 8.84. ^1H NMR (CD_2Cl_2, 400 MHz, 298 K, ppm): δ 7.67 (t, $J = 7.8$ Hz, 2H, C_5H_3N); 7.35 (d, $J = 7.8$ Hz, 2H, C_5H_3N); 7.30 (d, $J = 7.8$ Hz, 2H, C_5H_3N); 5.88 (d, $J = 13.6$ Hz, 4H, C_4H_2N); 5.79 (d $J = 9.2$ Hz, 4H, C_4H_2N); 5.04 (m, 2H, CH_2); 3.56 (d, $J = 24.8$ Hz, 2H, C_4H_2N); 3.45 (d, $J = 24.8$ Hz, 2H, C_4H_2N); 3.11 (m, 2H, CH_2), 2.87 (m, 2H, CH_2); 2.57 (m, 4H, CH_2); 2.42 (m, 6H, CH_2); 2.27 (m, 6H, CH_2); 2.17 (m, 6H, CH_2); 1.92 (m, 2H, CH_2); 1.82 (m, 2H, CH_2); 1.09 (t, 12H, CH_3); 0.96 (t, 10H, CH_3); 0.89−0.74 (m, 18H, CH_3); 0.70 (t, 8H, CH_3). The synthesis of **9** was equally well carried out mixing an equimolar amount of **6** and **8** in thf, then following the procedure above (99%).

Synthesis of 10. $LiBu^n$ (4 mL, 1.6 in *n*-hexane, 6.4 mmol) was added dropwise to an orange-red solution of **9** (3.84 g, 3.2 mmol) in THF (120 mL). The solution turned amber. At the end of the addition, the solution was refluxed for 3 h, then the solvent was evaporated and the resulting yellow solid collected with *n*-hexane (80 mL), filtered and dried (4.7 g; 88%). Anal. Calcd for **10**, $C_{90}H_{128}Li_2N_8Ni_2O_4$: C, 71.24; H, 8.50; N, 7.38. Found: C, 70.93; H, 8.21; N, 7.15. ^1H NMR (CD_2Cl_2, 200 MHz, 298 K, ppm): δ 6.98 (s br, 6H, C_5H_3N); 6.40 (s, 2H, C_4HN); 6.18 (s br, 8H, C_4H_2N); 3.94−3.11 (s br, 12H, CH_2); 3.36 (m, 16H, THF); 2.78−1.82 (s br, 20H, CH_2); 1.36 (m, 16H, THF); 1.35−0.81 (s br, 48H, CH_3).

Synthesis of 11. $[Cp_2FeBPh_4]$ (5.15 g, 10.2 mmol) was added to a yellow solution of **2** (3.64 g, 5.1 mmol), cooled at −40 °C. The resulting red solution was kept at room temperature for 12 h. The solvent was evaporated, and the red solid was extracted with pentane

Table 1. Experimental Data for the X-ray Diffraction Studies on Crystalline Complexes **5**, **7**, **8**, **9**, and **11**

	5	**7**	**8**	**9**	**11**
empirical formula	$C_{37}H_{49}CoN_4 \cdot C_{16}H_{32}LiO_4$	$C_{45}H_{65}CuLiN_4O_2$	$C_{37}H_{49}N_4Ni \cdot C_{24}H_{20}B$	$C_{74}H_{98}N_8Ni_2 \cdot C_4H_{10}O$	$C_{41}H_{57}LiN_4O$
a, Å	16.320(5)	12.043(3)	14.275(3)	15.999(3)	11.815(2)
b, Å	20.671(6)	19.010(5)	14.482(3)	16.855(3)	15.941(3)
c, Å	15.276(4)	19.147(2)	12.745(2)	27.157(5)	11.261(2)
α, deg	90	90	100.19(2)	90	99.07(2)
β, deg	90	100.66(1)	101.47(2)	106.02(3)	113.88(3)
γ, deg	90	90	99.03(2)	90	71.87(2)
V, Å^3	5153(4)	4307.8(16)	2490.5(9)	7039(3)	1842(5)
Z	4	4	2	4	2
fw	904.1	764.5	927.8	1291.2	628.9
space group	$P2_12_12_1$ (No. 19)	$P2_1/n$ (No. 14)	$P\bar{1}$ (No. 2)	$C2/c$ (No. 15)	$P\bar{1}$ (No. 2)
t, °C	22	22	−130	22	−130
λ, Å	0.710 69	1.541 78	1.541 78	0.710 69	1.541 78
ρ_{calc}, g cm^{-3}	1.165	1.192	1.237	1.218	1.134
μ, cm^{-1}	3.75	9.77	8.54	5.85	4.83
transm coeff	0.679−1.000	0.875−1.000	0.762−1.000	0.952−1.000	0.540−1.000
R[a]	0.063 [0.064][b]	0.060	0.072	0.037	0.064
wR2[c]	0.189 [0.193]	0.192	0.219	0.092	0.197

[a] $R = \sum|\Delta F|/\sum|F_o|$ calculated on the unique observed data [$I > 2\,\sigma(I)$]. [b] Values in brackets refer to the "inverted" structure. [c] $wR2 = [\sum w|\Delta F^2|^2/\sum w|F_o^2|^2]^{1/2}$ calculated on the unique data having $I > 0$.

to remove impurities. The residue was collected with benzene (100 mL) and stirred for 1 h. Dioxane (∼50 mL) was then added to complete the precipitation of $LiBPh_4$, which caused the color to turn suddenly from yellow to purple red. $LiBPh_4$ was filtered off, the solvent evaporated to dryness, and the orange solid was collected with *n*-hexane (70 mL), filtered, and dried (1.9 g; 61%). Crytsal suitable for X-ray analysis were grown in THF/heptane. Anal. Calcd for **11**, $C_{41}H_{57}LiN_4O$: C, 78.31; H, 9.14; N, 8.91. Found: C, 78.15; H, 8.76; N, 8.55. ^{1}H NMR (C_6D_6, 400 MHz, 298 K, ppm): δ 6.78 (bs, 3H, C_5H_3N); 6.74 (d, $J = 3.6$ Hz, 2H, C_4H_2N); 6.48 (d, $J = 4$ Hz, 2H, C_4H_2N); 6.44 (s, 2H, C_4H_2N); 3.57 (m, 4H, THF); 2.56 (m, 2H, CH_2); 2.44−2.27 (m, 8H, CH_2); 2.19 (m, 2H, CH_2); 1.85 (m, 4H, CH_2); 1.41 (m, 4H, THF); 0.93 (m, 18H, CH_3); 0.72 (t, 6H, CH_3).

X-ray Crystallography for Complexes 5, 7−9, and 11. Suitable crystals were mounted in glass capillaries and sealed under nitrogen. Reduced cells were obtained with the use of TRACER.[5] Crystal data and details associated with data collection are given in Tables 1 and S1. For complex **9** data were collected at 293 K on a Stoe IPDS area detector. A total of 200 images from $\varphi = 0°$ to $\varphi = 180°$ were recorded, each one exposed for 240.8 s. The diffraction data were indexed and processed using the STOE program package. No absorption correction was deemed necessary. Data for complexes **5**, **7**, **8**, and **11** were collected on a Rigaku AFC6S single-crystal diffractometer at 295 K for **5** and **7** and 133 K for **8** and **11**. For intensities and background, individual reflection profiles were analyzed.[6] The structure amplitudes were obtained after the usual Lorentz and polarization corrections,[7] and the absolute scale was established by the Wilson method.[8] For **5**, **7**, **8**, and **11** the crystal quality was tested by ψ scans showing that crystal absorption effects could not be neglected. Data were then corrected for absorption using a semiempirical method.[9] The function minimized during the least-square refinements was $\sum w(\Delta F^2)^2$. Anomalous scattering corrections were included in all structure factor calculations.[10b] Scattering factors for neutral atoms were taken from ref 6a for nonhydrogen atoms and from ref 11 for H.

Structure solutions were based on the observed reflections [$I > 2\sigma(I)$], while the refinements were solved by the heavy-atom method starting from a three-dimensional Patterson map.[12] Refinements were done by full-matrix least-squares, first isotropically and then anisotropically for all non-H atoms except for the disordered atoms. For all complexes the hydrogen atoms were located from difference Fourier maps and introduced in the refinements as fixed atom contributions ($U_{iso} = 0.10$, 0.12, 0.05, 0.08, and 0.05 Å^2 for **5**, **7**, **8**, **9**, and **11**, respectively). The H atoms associated with the disordered carbon atoms were ignored. In the last stage of refinement the weighting scheme $w = 1/[\sigma^2(F_o^2) + (aP)^2]$ (with $P = (F_o^2 + 2F_c^2)/3$ was applied with *a* resulting in the value of 0.1077, 0.1177, 0.0916, 0.0621, and 0.1112 for **5**, **7**, **8**, **9**, and **11**, respectively. All calculations were performed by using SHELX92.[13] The final difference maps showed no unusual features, with no significant peaks above the general background.

Refinements of complexes **8**, **9**, and **11** was carried out straightforwardly. In complex **5** the C(26), C(27) ethyl group was affected by disorder, which was solved by splitting the atoms over two positions, called A and B, isotropically refined with a site occupation factor of 0.6 and 0.4, respectively. Moreover the THF molecules of the $[Li(THF)_4]^+$ cation showed rather high thermal parameters indicating the presence of disorder. The best fit was obtained by splitting the O(1), C(41)−C(44), C(45), C(49), C(59) atoms over two positions, called A and B, isotropically refined with site occupation factors of 0.5. During the refinement the C−C and C−O, bond distances within the disordered ethyl group and THF molecules were constrained to be 1.54(1) and 1.48(1) Å, respectively. Since the space group is polar, the crystal chirality was tested by inverting all the coordinates ($x, y, z \rightarrow -x, -y, -z$) and refining to convergence again. The resulting *R* values ($R = 0.064$, $wR2 = 0.193$) indicated that the original choice should be considered the correct one.

In complex **7** the THF molecules bonded to the lithium cation were found to be affected by disorder, which was solved by splitting the C(42)−C(48) carbon atoms over two positions, called A and B, isotropically refined with site occupation factors of 0.5. During the refinement the C−C and C−O bond distances within the disordered THF molecules were constrained to be 1.54(1) and 1.48(1) Å, respectively.

Final atomic coordinates for non-H atoms and for hydrogens, thermal parameters, and bond distances and angles, are listed in Tables S2−S21.[14] Ordering information is given on any current masthead page.

(5) Lawton, S. L.; Jacobson, R. A. *TRACER (a cell reduction program)*; Ames Laboratory, Iowa State University of Science and Technology: Ames, IA, 1965.
(6) Lehmann, M. S.; Larsen, F. K. *Acta Crystallogr., Sect. A: Cryst. Phys., Diffr., Theor. Gen. Crystallogr.* **1974**, *A30*, 580−584.
(7) Data reduction was carried out on a Quansan personal computer equipped with an Intel Pentium processor and on an ENCORE 91 computer.
(8) Wilson, A. J. C. *Nature* **1942**, *150*, 151.
(9) North, A. C. T.; Phillips, D. C.; mathews, F. S. *Acta Crystallogr., Sect. A: Cryst. Phys., Diffr., Theor. Gen. Crystallogr.* **1968**, *A24*, 351.
(10) (a) *International Tables for X-ray Crystallography*; Kynoch Press: Birmingham, England, 1974; Vol. IV, p 99. (b) *International Tables for X-ray Crystallography*; Kynoch Press: Birmingham, England, 1974; Vol. IV, p 149.
(11) Stewart, R. F.; Davidson, E. R.; Simpson, W. T. *J. Chem. Phys.* **1965**, *42*, 3175.
(12) Sheldrick, G. M. *SHELX76: Program for Crystal Structure Determination*; University of Cambridge: Cambridge, England, 1976.
(13) Sheldrick, G. M. *SHELXL92: Program for Crystal Structure Refinement*; University of Göttingen: Göttingen, Germany, 1993.

Scheme 1

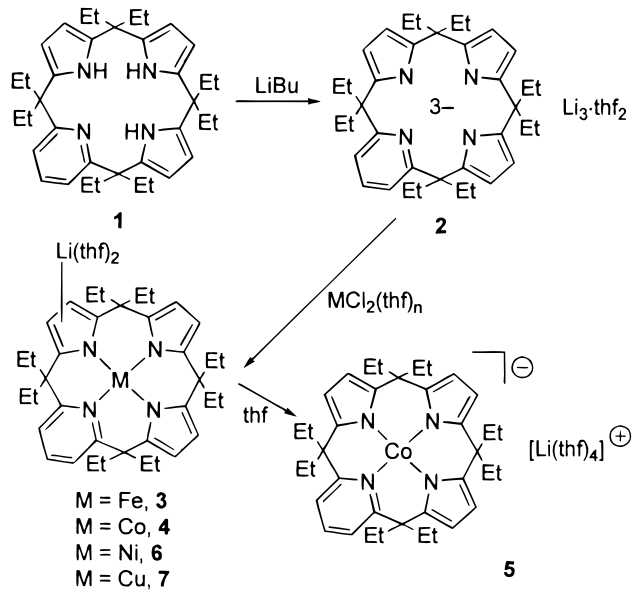

Results and Discussion

The porphyrinogen modified skeleton **1** has been obtained by the Zr-assisted homologation of the porphyrinogen skeleton according to the published procedure summarized in Chart 1.[4b] The metalation of **2** has been carried out via its deprotonation[4b,15] with LiBu was followed by the reaction with the metal halide (Scheme 1). Complexes **3**, **4**, **6**, and **7** occur in a bimetallic form, with the transition metal within the N_4 core and lithium cation η^5-bonded to one of the pyrroles. In solution or under different crystallization conditions, such complexes can exist in the separated ion-pair form, as it was the case of cobalt, see complex **5** in Scheme 1. The proposed structures are supported by an X-ray analysis carried out on **5** and **7**.

Selected bond distances and angles for complexes **5**, **7**-**9**, and **11** are given in Table 2. In Table 3 are quoted the most relevant conformational parameters for all complexes. The pyrrole rings containing N(1), N(2), and N(3) are labeled A, B, and C, respectively. The pyridine ring containing N(4) is labeled D. The numbering scheme of the ligand is given in Chart 2.

The structure of **5** consists of discrete $[Et_8(C_5H_3N)(C_4H_2N)_3Co)]^-$ anions (Figure 1) and $[Li(THF)_4]^+$ cations in the stoichiometric molar ratio of 1/1. Cobalt exhibits a slightly distorted square planar coordination provided by the nitrogen atoms of the trispyrrole−monopyridine ligand. The N_4 core shows small but significant tetrahedral distortions from the planarity, the deviations ranging from −0.036(8) to 0.033 Å for N(2) and N(3), respectively (Table 3). The metal atom deviates from the mean plane through the donor atoms by 0.028(1) Å. The Co−N bond distances to the nitrogen atoms of the pyrrole rings [mean value 1.884(9) Å] are shorter than the Co−N(4) bond distance to pyridine [1.994(6) Å]. The macrocycle assumes the usual saddle-shape conformation with the pyrrole and pyridine rings tilted on the same side with respect to the N_4 core. The differences observed in the dihedral angles between the N_4 mean plane and the A, B, C, D rings are rather small (Table 3) and could be related to the asymmetry of the molecule induced by the pyridine ring. The conformation of the ligand leads two methylene carbon atoms [C(26), C(34)] above and two [C(24), C(32)] below the coordination plane providing a flattened tetrahedral cage for the cobalt atom. In this orientation a hydrogen atom for each methylene group points toward the metal at distances ranging from 2.32 to 2.83 Å.

The structure of **7** consists of discrete $[Et_8(C_5H_3N)(C_4H_2N)_3Cu\{Li(thf)_2\}]$ units (Figure 2), in which a $[Li(THF)_2]^+$ cation is anchored to the B pyrrole ring of a $[Cu(Et_8N_3Py)]^-$ anion. The range of the Li-N [2.650(11) Å] and Li−C distances [from 2.253(13) to 2.519(13) Å] suggests a Li^+−pyrrole η^5-interaction. As observed in **5**, the N_4 core shows small but significant tetrahedral distortions from the planarity [the deviations ranging

Table 2. Selected Bond Distances (Å) and Angles (deg) for Complexes **5**, **7**, **8**, **9**, and **11**[a]

	5	**7**	**8**	**9**	**11**
M−N(1)	1.879(6)	1.883(4)	1.860(7)	1.851(2)	2.309(6)
M−N(2)	1.903(7)	1.951(4)	1.874(8)	1.894(2)	2.201(7)
M−N(3)	1.873(7)	1.895(4)	1.822(7)	1.852(2)	2.059(8)
M−N(4)	1.994(6)	2.119(4)	1.933(7)	1.960(2)	2.767(8)
N(1)−C(1)	1.369(10)	1.374(5)	1.294(11)	1.358(3)	1.331(4)
N(1)−C(4)	1.368(12)	1.372(6)	1.449(11)	1.371(4)	1.431(4)
N(2)−C(6)	1.377(14)	1.373(6)	1.425(11)	1.459(4)	1.432(4)
N(2)−C(9)	1.356(14)	1.373(6)	1.307(11)	1.302(3)	1.315(5)
N(3)−C(11)	1.390(12)	1.394(6)	1.400(12)	1.370(3)	1.379(4)
N(3)−C(14)	1.352(12)	1.359(6)	1.365(12)	1.369(4)	1.378(5)
N(4)−C(16)	1.397(10)	1.352(6)	1.360(11)	1.376(3)	1.332(6)
N(4)−C(20)	1.387(10)	1.349(6)	1.414(12)	1.364(3)	1.352(4)
C(4)−C(6)			1.570(13)		1.639(5)
C(7)−C(7′)				1.476(5)	
N(3)−M−N(4)	90.4(3)	89.8(2)	94.9(3)	90.4(1)	83.8(2)
N(2)−M−N(4)	176.3(3)	177.0(2)	174.5(3)	176.4(1)	138.8(3)
N(2)−M−N(3)	88.3(3)	88.8(2)	89.8(3)	88.9(1)	92.3(3)
N(1)−M−N(4)	91.5(3)	90.4(2)	92.0(3)	91.4(1)	80.5(2)
N(1)−M−N(3)	178.1(3)	178.1(2)	171.8(3)	177.9(1)	142.3(3)
N(1)−M−N(2)	89.8(3)	91.1(2)	83.1(3)	89.2(1)	77.9(2)
M−N(1)−C(4)	129.0(6)	126.7(3)	120.3(6)	127.7(1)	112.3(4)
M−N(1)−C(1)	123.4(5)	124.7(3)	123.7(5)	123.4(2)	122.7(4)
C(1)−N(1)−C(4)	107.4(7)	108.1(4)	107.3(7)	107.9(2)	105.3(4)
M−N(2)−C(9)	125.6(6)	124.4(3)	128.2(6)	124.9(2)	113.3(4)
M−N(2)−C(6)	125.8(6)	125.0(3)	118.0(6)	125.3(1)	116.9(4)
C(6)−N(2)−C(9)	107.4(8)	108.8(4)	107.6(7)	109.4(2)	106.7(4)
M−N(3)−C(14)	123.8(6)	125.2(3)	123.7(6)	124.1(2)	130.7(4)
M−N(3)−C(11)	127.8(6)	127.4(3)	129.2(6)	127.5(2)	123.6(4)
C(11)−N(3)−C(14)	108.0(8)	107.3(4)	106.9(7)	108.4(2)	105.3(4)
M−N(4)−C(20)	121.0(5)	119.6(3)	121.4(5)	120.1(2)	114.1(4)
M−N(4)−C(16)	120.3(5)	118.4(3)	121.1(6)	120.7(1)	108.3(4)
C(16)−N(4)−C(20)	118.3(6)	119.4(4)	117.2(6)	118.9(2)	119.4(5)
C(5)−C(4)−C(6)			59.0(5)		56.4(3)
C(4)−C(5)−C(6)	109.2(7)	110.8(4)	61.4(5)	105.4(2)	65.8(3)
C(4)−C(6)−C(5)			59.5(5)		57.8(3)

[a] M should be read as Co, Cu, Ni, and Li for **5**, **7**, **8**, **9**, and **11**, respectively. In **9** a prime denotes a transformation of $-x, y, 0.5 - z$.

Chart 2. Labeling Scheme Adopted for the Porphyrinogen Macrocycle

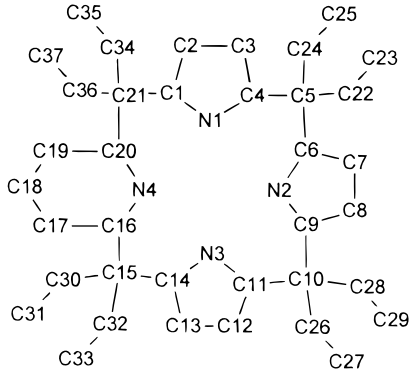

(14) See paragraph at the end of paper regarding Supporting Information.
(15) Crescenzi, R.; Solari, E.; Floriani, C.; Chiesi-Villa, A.; Rizzoli, C. *Organometallics* **1996**, *15*, 5456.

Table 3. Comparison of Relevant Structural Parameters within the Metal−Porphyrinogen Units for Complexes **5**, **7**, **8**, **9**, and **11**

distance of atoms from the N_4 core, Å	N(1)	0.023(6)	0.038(4)	−0.013(7)	0.020(2)	0.069(5)
	N(2)	−0.036(8)	−0.040(4)	0.013(7)	−0.021(2)	−0.076(5)
	N(3)	0.033(7)	0.039(4)	−0.012(7)	0.021(2)	0.064(5)
	N(4)	−0.028(7)	−0.037(4)	0.010(6)	−0.020(2)	−0.063(5)
	M[a]	0.028(1)	0.007(1)	0.054(2)	0.038(1)	0.763(7)
distance of M from A,[b] Å		0.093(1)	0.254(1)	0.801(2)	0.281(1)	1.499(7)
distance of M from B,[b] Å		0.324(1)	0.388(1)	0.750(2)	0.216(1)	1.627(7)
distance of M from C,[b] Å		0.089(1)	0.046(1)	0.065(2)	0.040(1)	0.250(7)
distance of M from D,[b] Å		0.431(1)	0.740(1)	0.266(2)	0.301(1)	1.998(7)
dihedral angles between the N_4 core and	(A)	148.2(3)	152.0(2)	140.6(3)	142.6(1)	120.7(1)
the A, B, C, D rings, deg	(B)	147.5(3)	148.4(2)	148.1(2)	146.5(1)	110.6(2)
	(C)	144.8(3)	145.0(1)	152.8(3)	143.6(1)	153.0(1)
	(D)	142.5(2)	140.6(1)	147.2(2)	139.8(1)	116.7(1)
dihedral angle between AB, deg		125.8(4)	136.6(2)	109.5(3)	119.6(1)	116.8(2)
dihedral angle between AD, deg		145.8(3)	140.0(2)	148.8(3)	144.4(1)	95.4(2)
dihedral angle between BC, deg		140.0(4)	143.0(2)	160.2(3)	139.4(1)	107.2(2)
dihedral angle between CD, deg		123.8(3)	116.8(2)	145.6(3)	120.2(2)	110.4(2)

[a] M should be read as Co(1) in **5**; Cu(1) in **7**; Ni(1) in **8** and **9**; and Li(1) in **11**. [b] A, B, C, and D define the pyrrole and pyridine rings containing the N(1), N(2), N(3), and N(4) nitrogen atoms, respectively.

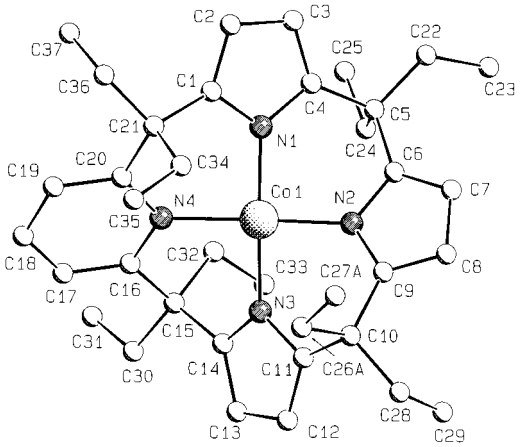

Figure 1. SCHAKAL view of the anion in complex **5**. Disorder has been omitted for clarity.

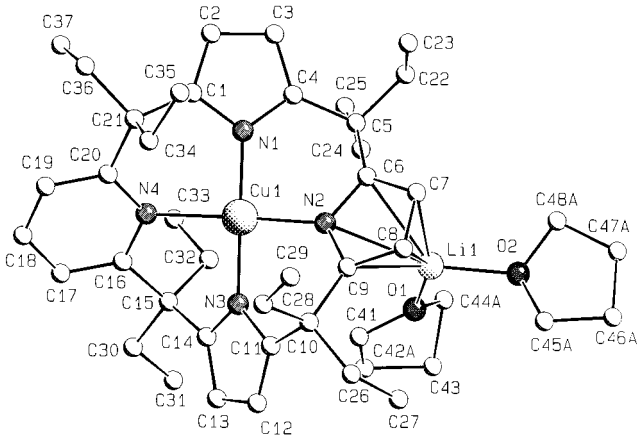

Figure 2. SCHAKAL view of complex **7**. Disorder has been omitted for clarity.

from −0.040(4) to 0.039(4) Å] providing a distorted square planar coordination to the copper atom. The metal deviates from the mean plane through the donor atoms by 0.007(1) Å (Table 3). The Cu−N bond distances to the nitrogen atoms N(1) and N(2) [mean value 1.889(6) Å] are significantly shorter than that to N(2) [1.951(4) Å], as a possible consequence of the anchorage of the lithium cation to the B ring. The Co−N(4) bond distance [2.119(4) Å] to pyridine is, as usual, longer. The structural parameters support the bond sequences given in Scheme 1. The macrocycle assumes the saddle-shape conformation similar to that observed in **5**, the main difference consisting in metal out-of-plane distance from the A ring (Table 3). The conformation of the ligand leads two methylene carbon atoms [C(28), C(34)] above and two [C(24), C(32)] below the coordination plane providing a flattened tetrahedral cage for the metal. Four hydrogen atoms, provided by the methylene, approach the metal at distances ranging from 2.31 to 3.14 Å. Coordination around the lithium cation is completed by the oxygen atoms from two THF molecules.

The major difference between the structures of **5** and **7** consists in the occurrence of **5** as an ion separated form, while **7** has an ion-pair structure. Although all compounds **3**, **4**, **6**, and **7** are obtained in the ion-pair form (see Experimental Section), the solvation to the ion-separated form can be relatively easy, and should be considered when we run the reaction in solution. This may be related to the nature of the transition metal affecting the basicity of the peripheral pyrroles. The magnetic properties of **3** and **4** are as expected from related complexes reported in the literature. In the case of **5**, the magnetic moment of 2.75 at 293 decreasing only slowly with the temperature, though anomalous, is currently found for square planar cobalt(II) complexes.[16] The behavior of **3** is quite similar to that of related square planar iron(II) in an N_4 environment such as, for example, the tetraphenylporphyrin or the phthalocyanine.[17]

The reported compounds **3**−**7** belong to two classes of compounds, those having a metal ion undergoing an easy redox chemistry, and the nickel derivative **6**, in which the metal would hardly change oxidation state in such a coordination environment. We explored the redox chemistry of **6** with the purpose of discovering the synthetic consequences of the introduction of a pyridine ring in the macrocycle. Depending on the Ni/Cp_2Fe^+ ratio, the results are significantly different and are summarized in Scheme 2. The oxidation with an excess of Cp_2FeBPh_4 led to the formation of a cyclopropane unit[3] across the pyrrolyl ring, thus forming complex **8**, which is a two-electron oxidation product. The use of 2 equiv of oxidant only led to a mixture of **9** and **10**. The best access to **10** has been made using 1 equiv of Cp_2FeBPh_4 *per* nickel complex **6**. The oxidative dimerization of **6** occurs via the C−C bond formation between the pyrrole β-carbons of two different units. Complex **9** should not be considered, however, an intermediate to **8**, which

(16) Kahn, O. *Molecular Magnetism*; VDC: New York, 1993.
(17) (a) Barraclough, C. G.; Martin, R. L.; Mitra, S.; Sherwood, R. C. *J. Chem. Phys.* **1970**, *53*, 1643. (b) Boyd, P. W. D.; Buckingham, D. A.; McMeeking, R. F.; Mitra, S. *Inorg. Chem.* **1979**, *12*, 3585.

Scheme 2

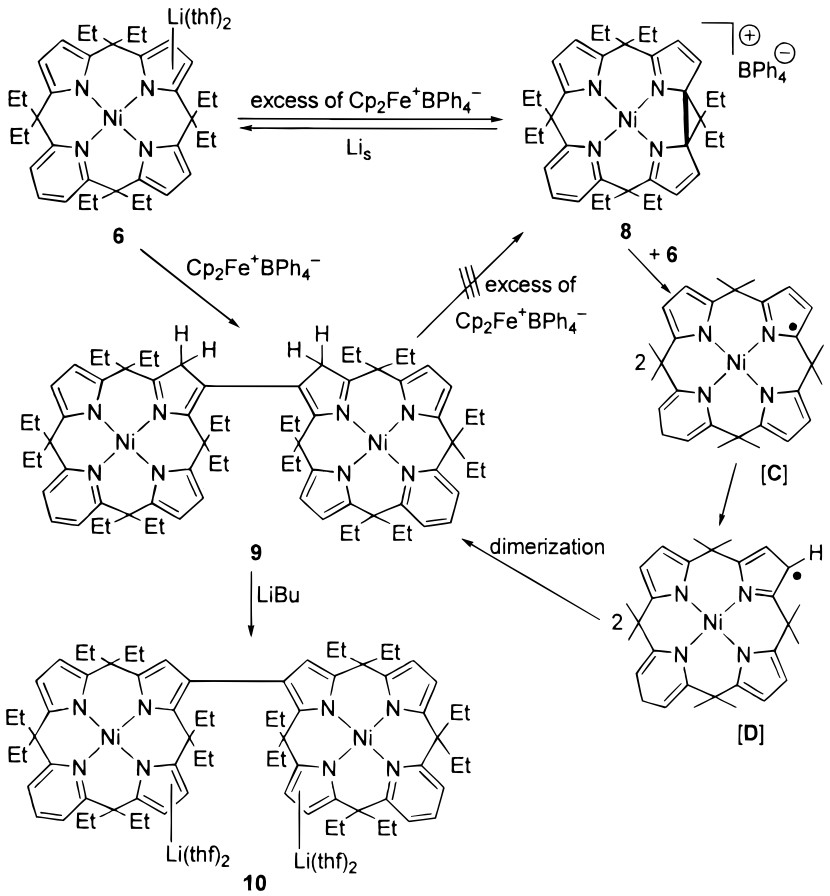

does not form from **9**, reacted with an excess of Cp_2FeBPh_4. The results mentioned here enable us to propose a plausible mechanism leading either to the intramolecular or intermolecular C−C bond formation. We should admit that the primary monoelectronic oxidation product should be the α-radical, as expected from the reactivity of the pyrrole, followed by a rather fast oxidation to the monocyclopropane derivative. Therefore, the formation of **9** would not occur via the rearrangement of the α- to the *β*-radical at the pyrrole ring. The former one would be intercepted by the oxidant before rearranging to the *β*, which couples intermolecularly to **9** which does not undergo conversion to **8** in the presence of an excess of oxidant. In addition, the high yield of **8** from the oxidation of **6** with an excess of Cp_2FeBPh_4, rules out two, intra- and intermolecular, parallel pathways. The answer to the question how complex **9** originates, comes from its formation from a reaction carried out mixing an equimolar amount of **6** and **8** in THF at room temperature. This reaction is particularly relevant for a number of aspects. First, it shows the ease of intermolecular electron transfer processes that we believed to be assisted by alkali cations, mainly lithium ion, which are able to bridge porphyrinogens in a different oxidation state,[3b,c] via rather strong ion−pyrrole interactions. Therefore, the formation of the two-electron oxidized form of the porphyrinogen containing a cyclopropane seems to precede any other oxidized forms. The reaction between **6** and **8** should produce the α-radicals [**C**] (see Scheme 2), which rearrange to the *β*-radicals [**D**], which finally couple to **9**. The formation and characterization of **8** and **9** allowed us to propose as plausible the free-radical pathway involving the formation of [**C**] to [**D**], though they have not been spectroscopically identified. The coupling reaction followed by the hydrogen shift to the C−C adjacent positions is quite general, namely in the acid−base chemistry of porphyrinogen.[18] The oxidative coupling of two Ni macrocycles to form a C−C joined dimer has been observed in the oxidation of [Ni(tmtaa)] [tmtaa = dibenzotetramethyltetraaza[14]annulene].[19]

In the case of **8** the reaction with lithium or sodium metals led to the reductive cleavage of the cyclopropane unit[3b,c] and the formation of the original monoanion **6** associated either with lithium or sodium cation, while in the case of **9** the reduction did not afford the cleavage of the C−C bond. In the latter case, rather we observed the deprotonation of **9**, a reaction which has been much easily achieved using LiBu. As a matter of fact, **9** was cleanly deprotonated to **10** using LiBu.

The reactions in Scheme 2 show an important synthetic consequence of the one-electron oxidation of the porphyrinogen-derived anions, namely the oxidative coupling leading to C−C bond linked dimers. The results reported in this section serve to clarify the role of the transition metal and the oxidizing agent in driving the oxidation of the macrocyclic trianion. Under the conditions of using an innocent oxidant, namely Cp_2FeBPh_4, monocyclopropane forms. However, in the case of transition metals we have to distinguish between metals which usually do not change oxidation state in the coordination environment determined by the porphyrinogen-type skeleton, i.e. Ni(II), and those which have different easily accessible oxidation states. In the latter case, the stepwise formation of cyclopropane is assisted by the one-electron redox chemistry at the metal and

(18) Bonomo, L.; Solari, E.; Floriani, C.; Chiesi-Villa, A.; Rizzoli, C. Submitted for publication.

(19) (a) Mountford, P. *Chem. Soc. Rev.* **1998**, *27*, 105. (b) Dabrowiak, J. C.; Fisher, D. P.; McElroy, F. C.; Macero, D. J. *Inorg. Chem.* **1979**, *18*, 2304 and references therein. (c) Bailey, C. L.; Bereman, R. D.; Rillema, D. P. *Inorg. Chem.* **1986**, *25*, 3149 and references therein.

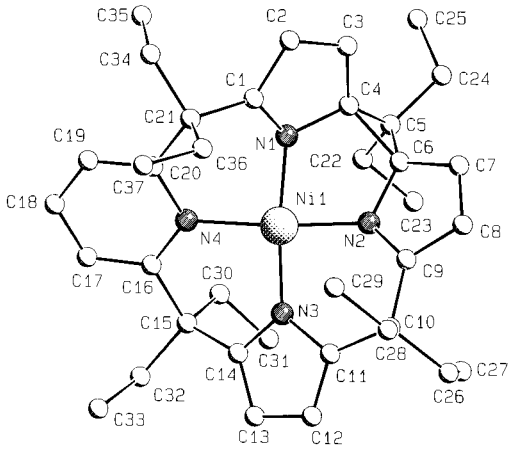

Figure 3. SCHAKAL view of the cation in complex **8**.

we do not really achieve and see the overall one-electron oxidation of the porphyrinogen.[3b,c] In the case of nickel, the overall one-electron oxidation, through the mechanism outlined above, leads to oxidative C−C coupling between two metallamacrocycle moieties. This is a quite important pathway, which, coupled with the deprotonation reaction,[18] will allow the formation of dimeric, oligomeric, and polymeric metallaporphyrinogen-type complexes. Compounds in Scheme 2 have been fully characterized (see the Experimental Section) including the X-ray analysis on **8** and **9**.

The structure of **8** consists of discrete $[Et_8(C_5H_3N)(C_4H_2N)_3(\Delta)Ni]^+$ cations (Figure 3) and $[B(Ph)_4]^-$ anions. The overall geometry of complex **8** differs mainly from those of **5** and **7** in the following parameters: (i) a small but significant lengthening of the Ni−N(1) and Ni−N(2) bond distances [mean value 1.866(9) Å], involving the nitrogen atoms of the A and B pyrrole rings forming the cyclopropane unit (Table 2) with respect to the Ni−N(3) bond distance [1.822(7) Å]; (ii) a larger deviation of the metal from the N_4 core [0.054(2) Å], which is planar within the experimental errors (Table 3); (iii) larger displacements of the metal from the A and B pyrrole rings. The bond distances within the A and B rings are consistent with a double bond localization on the N(1)−C(1), N(2)−C(9), C(2)−C(3), C(7)−C(8) bonds and with a single bond character for the N(1)−C(4), N(2)−C(6) distances and for the C−C distances adjacent to the macro-ring [C(1)−C(2), C(3)−C(4), C(6)−C(7), C(8)−C(9)]. The cyclopropane unit has the expected geometry.[3b,c] The configuration at the C(4) and C(6) asymmetric carbon atoms is *S*, *R* respectively with reference to the coordinates of Table S4. Since the space group is centrosymmetric, the enantiomeric diastereoisomer is present in the stucture. The conformation of the whole molecule is also different from that of complexes **5** and **7** for the orientation of the ethyl groups. Three methylene groups [C(22), C(30), C(36)] and one methyl group [C(29)] are arranged around the N_4 core providing a flattened tetrahedral cage for the metal. One hydrogen for each methylene group approaches the metal at distances ranging from 2.53 to 3.02 Å, while the remaining Ni···H contacts involving two hydrogen atoms from the methyl group are longer than 3.36 Å.

Complex **9** with a C_2 symmetry is shown in Figure 4. In addition the migration of the hydrogen atom from the C(7) to the adjacent C(8) carbon atom is observed, as is indicated by the values of bond distances and angles involving the C(7) and C(8) carbon atoms, which are in agreement with the sp^2 and sp^3 character respectively. The N_4 core shows small but significant tetrahedral distortions from the planarity, the deviations ranging from −0.021(2) to 0.021 Å for N(2) and N(3),

Scheme 3

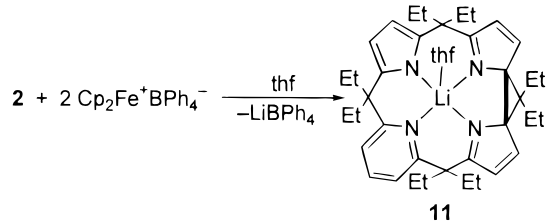

respectively (Table 3). The metal atom deviates from the mean plane through the donor atoms by 0.038(1) Å. As observed in **8**, the Ni−N(2) bond distance [1.894(2) Å] involving the B pyrrole ring forming the interligand C−C bond is slightly, but significantly, longer than those involving the negatively charged A and C rings (mean value 1.852(1) Å). The Ni−N(4) bond distance [1.960(2) Å] involving the pyridine ring is just significantly shorter than that observed in **8** [1.933(7) Å]. The structural parameters support the bonding sequence shown in Scheme 2. The overall geometry of the macrocycle is comparable with that observed in complex **5**, the main difference consisting in the out-of-plane distance of the metal from the A ring (Table 3). The conformation of the ligand leads two methylene carbon atoms [C(22), C(30)] above and two [C(28), C(36)] below the coordination plane, providing a flattened tetrahedral cage for the metal. One hydrogen atom from each methylene group approaches the metal at distances ranging from 2.42 to 2.96 Å.

The formation of a transition-metal-free oxidized form of *meso*-octaalkylporphyrinogen or analogous can create severe synthetic difficulties if demetallation is a compulsory choice. In the case of the *meso*-octaethyl mono(pyridine)−tris(pyrrole) the oxidation can be carried out equally well on the lithium derivative **2** (see Scheme 3). The oxidation with 2 equiv of Cp_2FeBPh_4 led to the formation of the corresponding cyclopropane derivative **11**, whose structure is shown in Figure 5.

The coordination polyhedron around the alkali metal can be described as distorted square pyramid, the nitrogen atoms of the N_4 core defining the base and the O(1) atoms from the THF molecule forming the apex. The N_4 core is significantly tetrahedrally distorted [the deviations from the planarity ranging from −0.076(5) to 0.069(5) Å] with the metal remarkably out of the mean plane by 0.763(7) Å toward the oxygen atom. The Li−O(1) vector forms a dihedral angle of 4.9(2)° with the normal to the mean plane through the N_4 core. As observed in **8** and **9**, the Li−N bond distances, involving the neutral nitrogen atoms of the A and B pyrrole rings bridged by the cyclopropane unit, are significantly longer [Li−N(1), 2.309(6) Å; Li−N(2), 2.201(7) Å] than those involving the negatively charged C pyrrole ring. The Li−N(4) [2.767(8) Å] is unusually very long, thus being at the limit of being considered as a bond distance. The structural parameters support the bonding sequence shown in Scheme 3. The C(4)−C(6) bond distance [1.639(5) Å] falls in the upper range of values observed for metal porphyrinogens containing cyclopropane units.[3b,c] The configuration at the C(4) and C(6) asymmetric carbon atoms is respectively with reference to the coordinates of Table S6. Since the space group is centrosymmetric the enantiomeric diastereoisomer is present in the structure. The formation of the the cyclopropane unit as well as the coordinative requirements of the alkali metal causes relevant differences in the structural parameters if compared with those of complex **8**. In particular the A, B, and D rings appear to be more bent with respect to the N_4 core (Table 3), giving rise to a calixarene-like conformation of the macrocycle. In this conformation the ligand points four hydrogen atoms

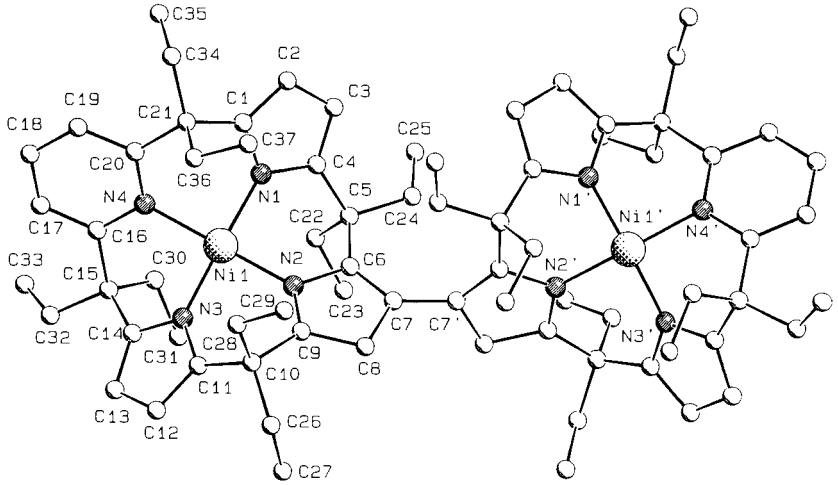

Figure 4. SCHAKAL view of complex **9**. A prime denotes a transformation of $-x$, y, $0.5 - z$.

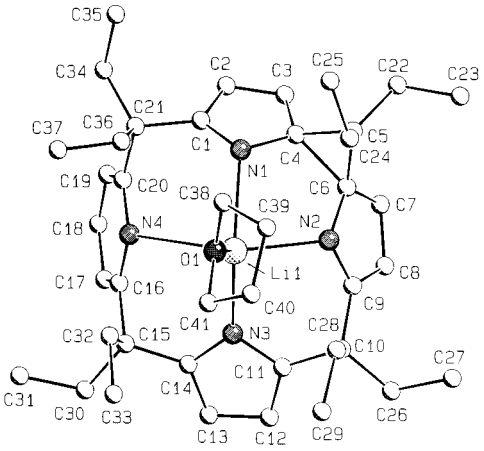

Figure 5. SCHAKAL view of complex **11**.

[H(242), H(282), H(321), H(361)] from the C(24), C(28), C(32), and C(36) *meso*-methylene carbons towards the oxygen atom of the THF molecule, the geometry of the interactions being: H(242)···O(1), 3.09 Å; C(24)−H(242)···O(1), 167°; H(282)···O(1), 2.71 Å; C(28)−H(282)···O(1), 174°; H(321)···O(1), 2.65 Å; C(32)−H(321)···O(1), 165°; H(361)···O(1), 2.64 Å; C(36)−H(361)···O(1), 161°.

The formation of **11** indicates that the oxidation of the porphyrinogen and porphyrinogen analogous towards the formation of cyclopropane can occur without the assistance of a transition metal ion. In addition, such a reaction makes the oxidized form available for the complexation of any kind of transition metal. A further consideration at this stage is the fact that the oxidation of porphyrinogen and porphyrinogen analogues containing hydrogen atoms, in the meso positions or within the N_4 core, leads exclusively to the aromatization of the N_4 macrocycle to porphyrin[3a,4b,20−22] or porphyrin analogues. In the case of *meso*-octaalkylporphyrinogen or *meso*-octaalkyl mono(pyridine)−tris(pyrrole) in their deprotonated forms, the oxidation leads exclusively to the formation of C−C bonds either intramolecularly (see cyclopropane) or intermolecularly (see the formation of C−C bridged dimers). The major difference between the two processes is, in the former case the removal of both protons and electrons, and in the latter case the removal of electrons exclusively. Such a difference is also important in terms of the relative stability of the reduced and oxidized forms. Such a difference is very high in the case of porphyrinogen−porphyrin,[3a,4b,d−f,19−21] while the interconversion between *meso*-octaalkylporphyrinogen and the corresponding oxidized form is quite easy.[3]

Conclusions

In this report we showed that the oxidative transformation of porphyrinogen analogues in the absence of protons either in the *meso*-positions and within the N_4 core, led to the formation of C−C bonds either intramolecularly or intermolecularly. In the former case the formation of cyclopropane units have been observed both in the presence and in the absence of transition metals. The synthesis of a metal-free cyclopropane derivative opens up perspectives for its use in the complexation of any kind of transition metal. This is particularly relevant because cyclopropane functions as a shuttle for two electrons. The formation of intermolecular C−C bonds showed the synthetic methodology for acceding to the formation of dimer and, eventually, oligomer of the porphyrinogen skeleton.

Acknowledgment. We thank the Fonds National Suisse de la Recherche Scientifique (Grant No. 20-40268.94) and Ciba-Geigy S.A. (Basel) for financial support.

Supporting Information Available: ORTEP and SCHAKAL drawings, and tables of crystallographic data for **5**, **7**−**9**, and **11** (36 pages). Ordering information is given on any current masthead page.

IC9806378

(20) (a) *The Porphyrins*; Dolphin, D., Ed.; Academic Press: New York, 1978; Vols. I and II. (b) Smith, K. M. *Porphyrins and Metalloporphyrins*; Elsevier: Amsterdam, 1975.

(21) Mauzerall, D. The Porphyrinogens. In *The Porphyrins*; Dolphin, D., Ed.; Academic: New York, 1978; Vol. 2, Chapter 3.

(22) (a) Jubb, J.; Jacoby, D.; Floriani, C.; Chiesi-Villa, A.; Rizzoli, C. *Inorg. Chem.* **1992**, *31*, 1306. (b) Solari, E.; Musso, F.; Floriani, C.; Chiesi-Villa, A.; Rizzoli, C. *J. Chem. Soc., Dalton Trans.* **1994**, 2015. (c) Jacoby, D.; Isoz, S.; Floriani, C.; Chiesi-Villa, A.; Rizzoli, C. *J. Am. Chem. Soc.* **1995**, *117*, 2805.